

# A Role of Environmental Complexity on Representation Learning in Deep Reinforcement Learning Agents

Andrew Liu, Alla Borisjuk

---

---

## Abstract

The environments where individuals live can present diverse navigation challenges, resulting in varying navigation abilities and strategies. Inspired by differing urban layouts and the Dual Solutions Paradigm test used for human navigators, we developed a simulated navigation environment to train deep reinforcement learning agents in a shortcut usage task. We modulated the frequency of exposure to a shortcut and navigation cue, leading to the development of artificial agents with differing abilities. We examined the encoded representations in artificial neural networks driving these agents, revealing intricate dynamics in representation learning, and correlated them with shortcut use preferences. Furthermore, we demonstrated methods to analyze representations across a population of nodes, which proved effective in finding patterns in what would otherwise be noisy single-node data. These techniques may also have broader applications in studying neural activity. From our observations in representation learning dynamics, we propose insights for human navigation learning, emphasizing the importance of navigation challenges in developing strong landmark knowledge over repeated exposures to landmarks alone.

Keywords: Deep reinforcement learning; Representation learning; Navigation; Neural network population encoding; Landmark knowledge

## 1. Introduction

Navigation is a critical and complex skill that is essential for human and animal success in the world. It involves tracking one's position, understanding landmarks, recognizing routes, and acquiring survey knowledge [21] to plan a path towards a goal. Landmarks are salient features of the environment that can be used to locate or orient, and routes are familiar paths between locations, often incorporating landmarks. Survey knowledge, akin to a cognitive map, allows planning new routes and depends on integrating diverse information sources. Success in developing survey knowledge varies considerably between individuals [24].

There are many factors that can contribute to individual differences in navigation skill, with sex [19] and age [15] being well-studied aspects. The primary difference we focus on in this study is that of an individual's home environment, which can also have profound effects on navigation ability. Work from Barhorst-Cates et al. [1] explored differences in skill between participants from Salt Lake City (Utah, USA) with its regular, grid-like streets and participants from Padua (Veneto, Italy) with organic, maze-like streets. They generally found that individuals from Padua had better access to survey knowledge and better ability to use cues. The primary experimental protocol performed with humans we focus on is known as the Dual Solutions Paradigm (DSP) [12]. This task evaluates survey knowledge by first guiding participants on a standard route along the outside of a maze, and later assessing how often they attempt to find novel paths (shortcuts) between locations.

In this study, we apply deep reinforcement learning (RL) [23] to model the navigation learning process. Our dual objectives are to leverage human navigation understanding to construct a training

---

*Email addresses:* [aliu@math.utah.edu](mailto:aliu@math.utah.edu) (Andrew Liu), [borisyuk@math.utah.edu](mailto:borisyuk@math.utah.edu); Dept. of Mathematics, 155 E 1400 S, Salt Lake City, UT 84109, USA (Alla Borisjuk)

environment for artificial agents, and to develop tools for probing the representations that the agents learn. RL has been successfully applied to various complex navigation tasks, providing a robust challenge for testing agent capabilities [6, 16, 17]. Inspired by the DSP, we developed a simulated environment to train RL agents, modulating shortcut availability to abstractly reflect differences in environment complexity seen in Salt Lake City and Padua. We examined how variations in the “growing up” setting of an agent influenced learning dynamics and strategy development. Specifically, we focused on shortcut usage as a measure of learning and behavior, and drew correlations between performance and representation learning.

In past work, we successfully developed methods to analyze the neural network representations developed in navigating agents [9], and we continue building more analysis and exploration tools in the present work. Representations can be viewed as correlations between the state of the environment and the activity of the agent’s neural network. In other words, they act as an internal model of the world that the agent faces. We explored spatial representations recorded from individual nodes, inspired by place cells found in the hippocampal system [18]. We also examined landmark sensitive representations, motivated by the importance of landmark usage in human navigation. Beyond individual neural network nodes, we also looked at two representations found across populations of nodes. We find that looking at the activity of a population smooths over noise that individual node activities have, and can even lend context to better understand what those noisy activations encode. We suggest that similar techniques to ours may be useful in general to understand the activities of neural networks as well as neuronal firing rates in brains.

Our results show that different representations evolve at various training stages, with environmental complexity affecting learning dynamics nonlinearly. First, basic spatial maps in individual nodes (reminiscent of hippocampal place cells) develop early in training, while landmark sensitivity develops later, and a trajectory sensitive representation found at the population level continues to develop even after the RL algorithm has converged to a near-optimal policy. We also observe complex learning dynamics in landmark sensitivity. We find that frequent presentation of a salient cue leads to a stable encoding of the cue. However, if another agent is exposed to the cue less often but in a context of greater navigation difficulty, this stimulates the network to eventually learn to encode the cue more robustly than frequent presentation alone.

Building on these insights from artificial agents, we make extrapolations about human navigators from environments of different navigation difficulty levels performing the DSP task. We predict that individuals from environments with consistently available distal landmarks, like Salt Lake City, will have better landmark knowledge compared to counterparts from more complex environments like Padua when both groups have limited navigation experience. On the other hand, when looking at groups with more experience or higher skill levels, those from Padua, which presents greater navigational challenge, will have stronger landmark knowledge.

Lastly, we observed significant changes in learning efficiency in artificial agents triggered by small changes to the environment. This observation leads us to propose a modification to the DSP where a few demonstrations of shortcuts are given initially. We hypothesize that this adjustment would strongly boost the frequency of shortcut usage in those who might otherwise be route followers.

## 2. Methods

### 2.1. Reinforcement Learning

In this paper we train artificial agents with deep RL [23] to perform a navigation task. The overall set up and training approach are similar to those introduced in an earlier publication [9]. The agents are trained in an environment that can be defined as a Partially Observable Markov Decision Process (POMDP) defined by a  $(S, A, P, R, \Omega, O)$  tuple. At each time step  $t$ , the environment has state  $s_t \in S$  and gives a limited amount of information about that state to the agent in an observation  $o_t \in \Omega$ . The mapping  $O : S \rightarrow \Omega$  defines what information is given. The agent performs actions from a discrete action space  $a_t \in A$ , the state evolves according to a transition function  $P : S \times A \rightarrow S$ , and a reward  $r_t$  is given according to  $R : S \times A \rightarrow \mathbb{R}$ .

The agent learns a policy  $\pi_\theta(a_t|o_t, h_t) = \mathbb{P}[a_t = a|o_t = o, h_t = h]$  where  $h_t$  is a hidden state  $h_t \in \mathbb{R}^k$  used in a recurrent layer of the network. The policy is parameterized by a neural network

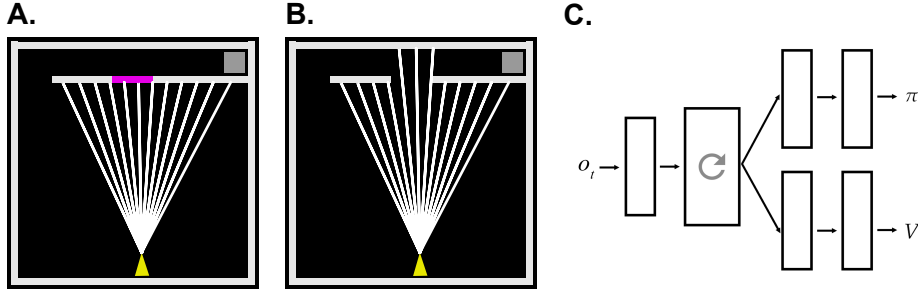


Figure 1: **A and B.** Depictions of the simulated shortcut navigation environment with **A.** shortcut closed and **B.** shortcut opened. All walls are colored white except for the shortcut wall when closed, which is purple. A gray box in the very top-right corner represents the navigation target. The agent is depicted as a yellow triangle, with white lines extending outwards its sight lines. **C.** A schematic of the neural network that agents are parameterized by. Each block represents network layer of 64 nodes, and the arrows represent the activations of one layer being passed to the next in a fully-connected weighted sum. The block with a circled arrow is a recurrent layer. Observation are input ( $o_t$  on the left of the schematic), and the network splits into actor ( $\pi$ ) and critic ( $V$ ) branches.

with parameters  $\theta$ . Simultaneously, the agent learns to predict expected return known as the value  $V(o_t, h_t) = \mathbb{E}^{\pi_\theta}[G_t | o_t, h_t]$ . The return  $G_t = \sum_{k=0}^{\infty} \gamma^k r_{t+k+1}$  is a discounted sum of future rewards, with discount factor  $\gamma \in [0, 1)$ .

## 2.2. The simulated navigation environment

In this study, we train agents to perform a 2D navigation task in Python, depicted in Fig 1A and 1B. The agent’s goal is to navigate to a target located in the top-right corner of the maze, represented as a gray box in the drawing. Sight lines (visualized in Fig 1) return both the color and distance to the wall each line intersects. This information forms a 24-dimensional observation vector  $o_t \in \Omega = \mathbb{R}^{24}$ , as each of the 12 vision lines provides two scalar values. At each time step, the agent picks from four possible actions  $a_t$ : a left or right turn of 0.2 radians, a forward movement of 10 units, or no movement. The navigation arena is a  $[0, 300] \times [0, 300]$  square.

The task is structured as an episodic RL task [23]. Each episode resets either when the agent reaches the goal or when 200 time steps elapse. If the goal is reached, a reward  $r_t$  of 1 is earned, and the reward is 0 for all other time steps. Upon resetting, the starting position of the agent is randomized such that the starting height is in  $[0, 240]$  to ensure that it starts below the corridor, which is the area above the maze’s long wall, 50 units high from the top edge. An initial direction is also selected uniformly at random in  $[0, 2\pi)$ .

This environment comes with a key parameter  $p$ , which determines the probability of the shortcut being open in any given episode. This parameter gives variations of the environment, and each agent is trained with a fixed  $p$  throughout all episodes. The state of the environment  $s_t$  is comprised of the agent’s location, direction, and whether the shortcut is open or not. After any initial randomizations of the state, the state evolves according to a deterministic transition function  $P$  that updates the agent’s location and heading based on the action  $a_t$  that it picks.

## 2.3. Agent network and training algorithm

Fig 1C shows a schematic of the artificial neural network that the agent is trained with. It is made up of primarily feed-forward layers, where the activation of one layer is propagated forward as a weighted sum to the next. The network splits into actor and a critic branches that output  $\pi$  and  $V$  respectively. The layer before the split is a gated recurrent unit [4], which is a recurrent layer that adds memory capabilities to the network, and is depicted with a circled arrow. Each layer in the network consists of 64 nodes. The agent accumulates training data by executing its policy in the environment and updates its neural network weights using a policy gradient method known as Proximal Policy Optimization (PPO) [8, 20]. Initially, each new agent starts with a randomly weighted neural network, leading to initially random actions. The output from the actor branch is a four-dimensional vector, transformed into a probability distribution over the four potential actions

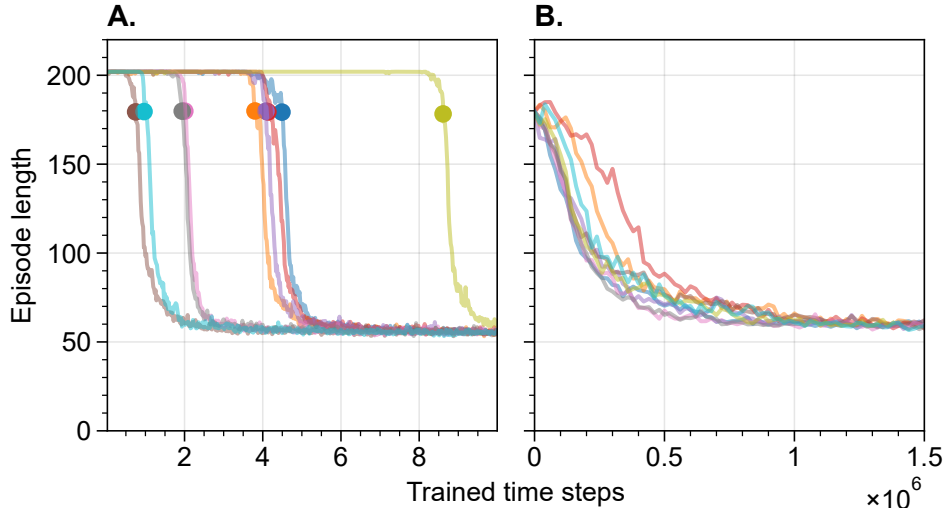


Figure 2: Examples of shifting learning curves, for agents trained with  $p = 0.1$ . Each line represents one agent. **A.** Original learning curves showing mean episode length for an agent. Dots depict where the mean first falls below 180. **B.** Learning curves shifted such that they start at the dots from **A.**

using a softmax function. The critic branch outputs a single scalar which is the agent’s predicted future return from the current state.

#### 2.4. Learning curves and initial non-learning periods

Learning curves, which graphically represent the performance of agents based on their cumulative experienced time steps, are shown in Fig 2A. These show mean episode length for individual agents, where an episode length of 200 means the time limit was reached before the agent made it to the target. At the start of training, agents perform random actions due to their randomly initialized neural networks. The first meaningful learning signals occur when agents accidentally reach the goal, from which they quickly learn to replicate successful actions. The learning curves show a steep increase in performance as the agents develop effective strategies at this point.

This pattern leads to an initial non-performant period which has random length, and its length does not impact learning dynamics afterwards. Since the shortcut path is shorter, it is easier for an agent taking random actions to reach the platform when the shortcut is open. Hence, agents trained with a higher probability  $p$  of the shortcut being open typically experience a shorter non-performant period. We disregard this initial variability by looking for the first time an agent’s average episode length drops below 180 time steps, shown by dots in Fig 2A. Fig 2B adjusts learning curves to start from this point, providing a clearer view of learning progression. Each agent undergoes training for  $6e6$  time steps beyond this initial point, and all results in this paper will use these shifted starting points.

#### 2.5. Evaluation episodes

To track agent performance and learning efficiency in a consistent manner, we employ a suite of standardized evaluation trials. First, we randomly generate 50 initial positions and directions, which are kept the same across evaluations. Agents are evaluated over 50 episodes with the shortcut open and another 50 with it closed, using these preset starting conditions. Evaluations occur at 36 predetermined checkpoints throughout training, beginning at the adjusted starting points described earlier. These checkpoints are more concentrated towards the beginning of training where performance changes most rapidly. At each checkpoint, a copy of the agent’s neural network is frozen and tested on the evaluation suite. This process of evaluating frozen copies of agents allows us to assess not only their navigational abilities, but also to later analyze the activations in their neural networks, which we use to explore learned representations.

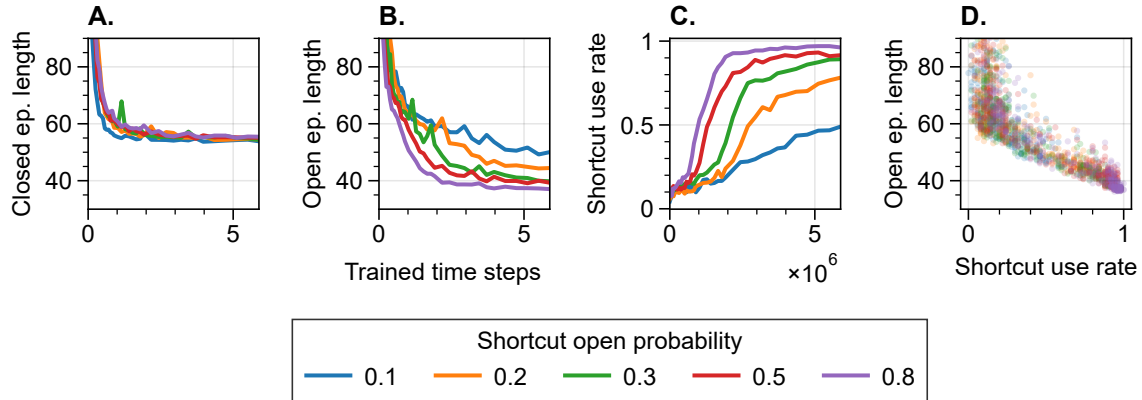


Figure 3: (A-C) Performance curves for agents trained with different  $p$  probabilities. **A.** Mean episode length on closed shortcut episodes. **B.** Mean episode length on open shortcut episodes. **C.** Mean shortcut use rate on open shortcut episodes. **D.** Shortcut use rate compared to episode length on open shortcut episodes, with each point representing one agent from one checkpoint.

### 3. Results

#### 3.1. Training conditions affect navigation ability

In this section, we begin by assessing how efficiently agents are able to learn the shortcut navigation task, with evaluation procedures detailed in the Methods section. Performance on closed and open shortcut episodes are shown in Fig 3A and Fig 3B respectively. A few key observations can be made from these plots. First, Fig 3A demonstrates that regardless of the value of  $p$ , agents rapidly achieve optimal performance in closed shortcut trials once initial learning signs appear. Agents with  $p = 0.1$  agents appear to reach an optimal policy slightly faster than others, likely due to more frequent exposure to closed shortcut episode. However, learning speeds in this condition for agents with  $p \geq 0.2$  are all roughly equivalent.

Fig 3B and C show navigation speed and shortcut use rate respectively on open shortcut episodes. Fig 3D confirms a clear correlation between the two. Agents trained in higher  $p$  environments gain more experience with open shortcut trials, directly influencing the speed at which they learn to use the shortcut consistently. Given enough training time, agents can learn to use shortcuts at a rate greater than the probability that they saw shortcuts during training. For instance,  $p = 0.1$  agents achieve around 50% shortcut usage by the end of training, and agents trained with  $p \geq 0.3$  all reach nearly 100% shortcut usage. Given an even longer training duration, it is possible that all agents could converge to fully optimal policies.

Performance on open shortcuts is the limiting factor for maximizing rewards, so the remainder of our analysis focuses on shortcut use rate as the primary measure of navigation learning in the simulated RL environment. In the following sections we analyze learned representations, building up our understanding of what agent networks learn in the navigation environment and how representations influence their performance.

#### 3.2. Position Representations

Representations can be thought of as encodings of environment state information within the activations of an artificial neural network layer [2, 10]. Using this definition, we may say that the neural network represents a  $d$ -dimensional vector feature  $x \in \mathbb{R}^d$  if there is a mapping  $\phi : \mathbb{R}^n \rightarrow \mathbb{R}^d$  that maps the  $n$  activations of a network layer to that feature. In practice, finding a formal mapping is impractical, so instead we focus on measuring the correlation between network activity and state or environmental information. Sometimes, we call the information about state a *feature* of the environment. When a strong correlation exists we consider the network activity to represent that feature.

Drawing inspiration from the hippocampal place cells and grid cells in the brain, which activate selectively based on spatial location [18], we initially explore position-based encodings in our artificial agents. These nodes help form a spatial representation of an agent’s position. We start by detailing our approach to computing these representations and then develop a measure of spatial representation strength. We discuss how having spatially consistent activations is necessary for basic navigation, but insufficient for advanced strategies. Then, we describe a technique that examines a population of nodes, giving us clearer insight into the spatial features that artificial agents tend to encode. This approach helps uncover representations which could otherwise be difficult to identify when looking at noisy activation patterns in individual nodes.

For all discussions of representations, we analyze activities in the recurrent layer of an agent’s neural network. This is the last layer in sequence that is shared between the actor and critic sides of the network. In principle, representations could be searched for in any layer of the neural network, and other works have performed representation analysis on for example, the penultimate actor layer [2]. Our focus remains on the recurrent layer due to its role in integrating and storing information, acting as the agent’s internal memory.

### 3.2.1. Spatial heatmaps and local variance measure

The first individual node level representations we present are spatial representations, examined by generating spatial activation heatmaps. While tasking agents with completing the 100 evaluation episodes outlined in Sec 3.1, we collect both the positions that agents were in and activations of their recurrent neural network layers at each time step. Heatmaps are generated by taking a Gaussian-weighted spatial average of these individual activation data points. We partition the maze space into a 30 x 30 grid, coloring each grid point by a spatially-weighted average of activations from a single node across all episodes. In other words, a heatmap illustrates how a node tended to activate when the agent was in different parts of the environment. Heatmaps are standardized to have zero mean and unit variance, highlighting deviations from a node’s typical outputs rather than absolute activation values. This gives us a clearer idea of what the node encodes.

Examples of some heatmaps are shown in Fig 4. These are chosen to be representative of common types of heatmaps observed in agents, but without preference for the  $p$  environment or point in training used. Some nodes show clear sensitivities for certain parts of the maze, such as corners (Fig 4A), the corridor (Fig 4B, E, G), nearby the corridor entrance (Fig 4C, D) or have a center-surround configuration (Fig 4F). They also range in amounts of noisiness, from what we might consider easy to interpret (Fig 4A-F) to noisy and difficult to interpret (Fig 4G-H).

To quantify the spatial representation strength of a node, we introduce a measure called the *mean local variance*. This measures the local consistency of activation patterns within the heatmap. As illustrated in Fig 5A, we calculate standard deviations for each 5x5 pixel window in the heatmap and average these to derive a single score for each node’s spatial representation. The score effectively captures the intuition that nodes with more consistent and interpretable spatial activations more strongly encode location information. It is likely that a single node is involved in the computation of multiple representations simultaneously, and a noisier heatmap may indicate a node that does not encode spatial information as much as other features. Note that while this score uses the standard deviation, we call it a local variance, but the two terms are equivalent in interpretation.

Fig 6A presents how the mean local variance measure evolves over training for  $p = 0.1$  agents, alongside the  $p = 0.1$  closed episode length performance curve from Fig 3A. We observe a sharp decline in both measures early in training as agents become proficient at navigation, followed by a plateau, suggesting no further improvement. A clear correlation between these two is shown in Fig 6B, and holds across all  $p$  agents. One may think of the closed shortcut performance curves as a proxy for basic navigation skill development since there is only one path to take, and navigation is relatively easy on these episodes. Spatial representation strength develops simultaneously with closed shortcut performance, suggesting that stable location encodings are crucial for basic navigation. We might similarly expect that in animals and humans, spatial consistency develops early in training, setting the foundation for other types of representations that mature more gradually.

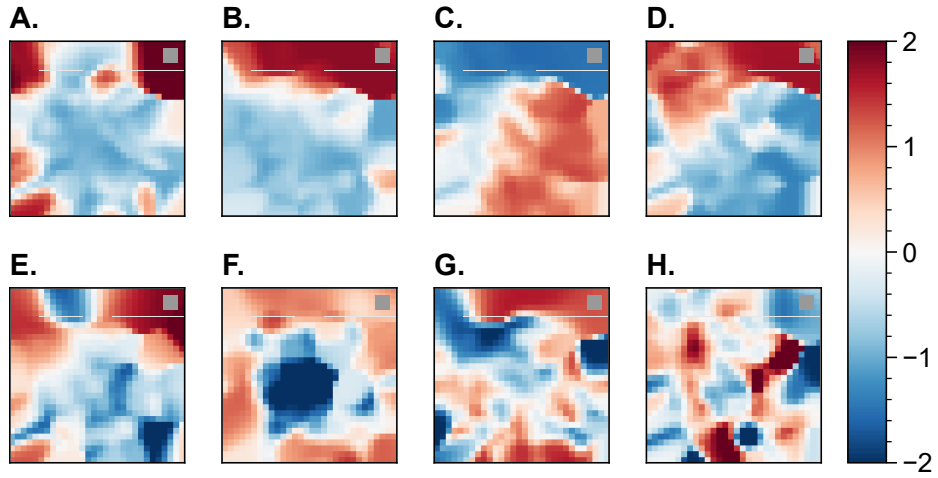


Figure 4: Examples of spatial heatmaps generated from agents at different points in training and taken from different  $p$  training environments. Each heatmap depicts a single node and how it typically activated based on the agent's location. Heatmaps have zero mean and unit variance, with red and blue indicating where a node had higher and lower than average activation respectively. Drawings of the goal and walls are also shown in each plot for reference.

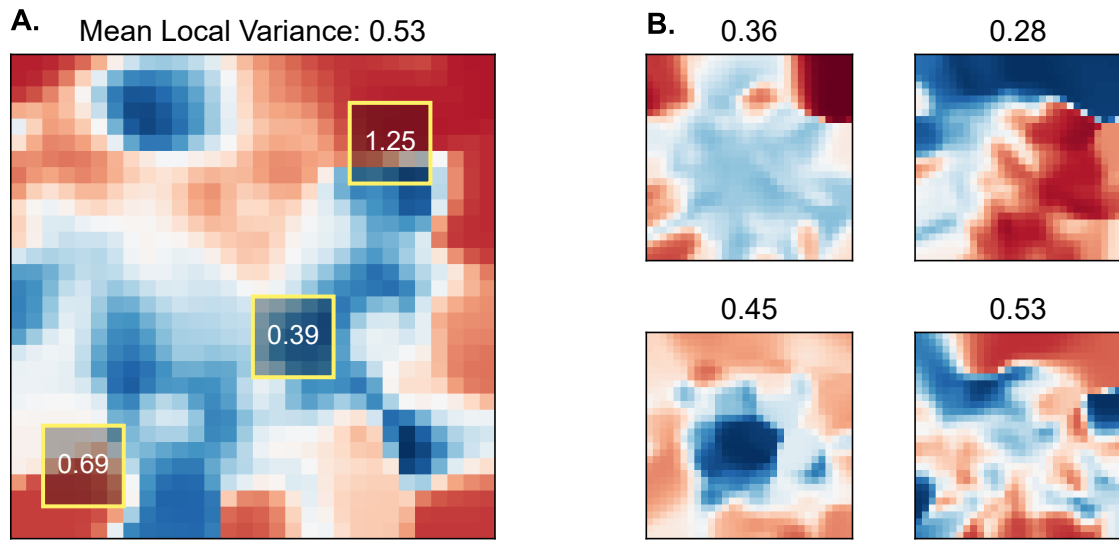


Figure 5: **A.** Yellow boxes show some example  $5 \times 5$  windows with the number inside giving the standard deviation of pixels inside. To get the mean local variance, we take the average of all standard deviations each possible  $5 \times 5$  window. **B.** Some example heatmaps with their corresponding mean local variances shown above.

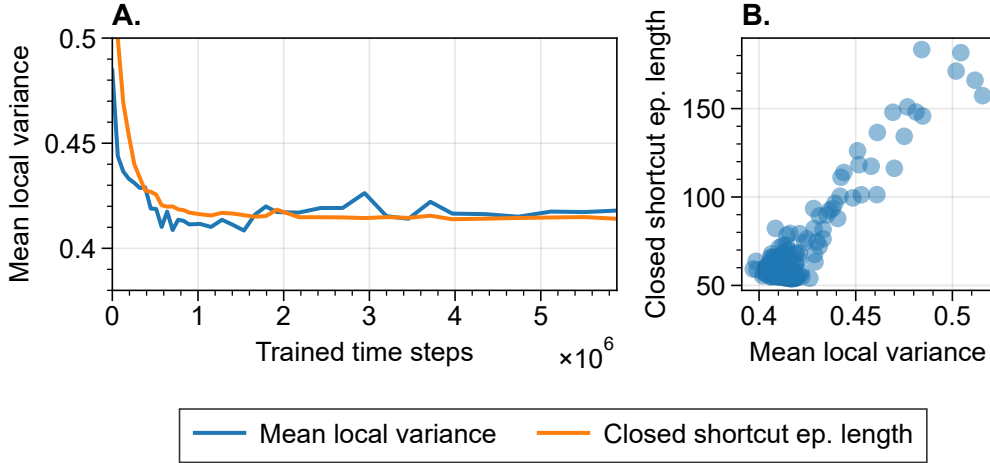


Figure 6: **A.** Mean local variance shown along with closed shortcut episode lengths for  $p = 0.1$  agents (agents trained with other  $p$  values have similar plots). Note that episode lengths in this subplot are shown with non-dimensional units and are shown just for comparison of time courses with the local variance measure. **B.** Correlation between mean local variance and closed shortcut episode lengths for all  $p$  agents. Each point represents one agent.

### 3.2.2. Clustering spatial heatmaps

Beyond quantifying the consistency of single node spatial representations, we are motivated in understanding what qualitative features nodes contribute to encoding. In order to do so, we demonstrate an effective technique of drawing signal out of the noise by looking at the features that whole populations of nodes encode. First, we take spatial heatmaps from every agent across all  $p$  values and 36 checkpoints, then apply k-means clustering with  $k = 12$ . This value of  $k$  tends to yield clusters with interpretable and distinct centers. Despite slight variations when running multiple iterations of k-means, the clustering algorithm also consistently settles on the same features. Notably, these clusters partition such that, when multiplying a cluster center by  $-1$  and inverting its sign, it approximates another cluster. This phenomenon is demonstrated in Fig 7 which depicts the cluster centers from one run of k-means, each of which can be visualized by a heatmap (the average of all heatmaps belonging to the cluster).

Note that the definitions of positive and negative clusters are arbitrary. For a given positive negative cluster pairing, the frequency of nodes being labeled as positive or negative are roughly equal, as depicted in Fig 8B. This relationship reflects the neural network’s ability to transmit the same information using activations whether they are above or below a node’s average.

Some features are clearly interpretable in the cluster centers of Fig 7. For example, clusters 1 and 2 are sensitive to the corridor of the maze. Cluster 3 extends this sensitivity to the long-path entrance to the corridor. Clusters 4 and 5 are sensitive to the top-right corner where the goal is located, suggesting of place-field-like encoding. Finally, cluster 6 looks like an edge-detection feature.

Fig 8A tracks these cluster frequencies across training, revealing stabilization early on for some clusters. Cluster 5 frequency (the cluster with clearest corner representation) starts the highest and drops off. Nodes in this cluster likely act as a place field for the goal, which may be important when the agent is first learning what the goal is. However, as the agent learns the routes to the goal, the utility of knowing the precise goal location decreases. Conversely, the frequency of nodes belonging to Cluster 3 that are sensitive to the long-path entrance see an increase over training, underscoring their navigational value.

Between different clusters, the ranges of local variances of nodes are mostly comparable, as shown in Fig 8C. We emphasize the relatively large range of local variances shown by the boxplots (See Fig 5 for some pictures of different variance scores). Every cluster contains nodes ranging from locally consistent to noisy. Despite the large variability of nodes inside each cluster, the clusters themselves are consistent when running k-means multiple times. This suggests that k-means effectively captures



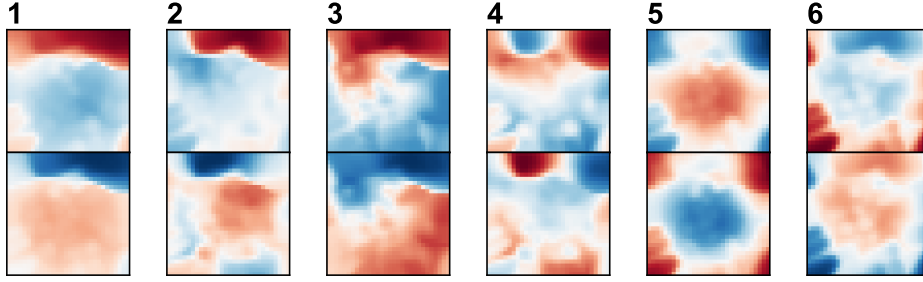


Figure 7: Cluster centers generated from one run of k-means with  $k = 12$  on spatial activation heatmaps. Each column shows one “positive” cluster center with its closest negative below it.

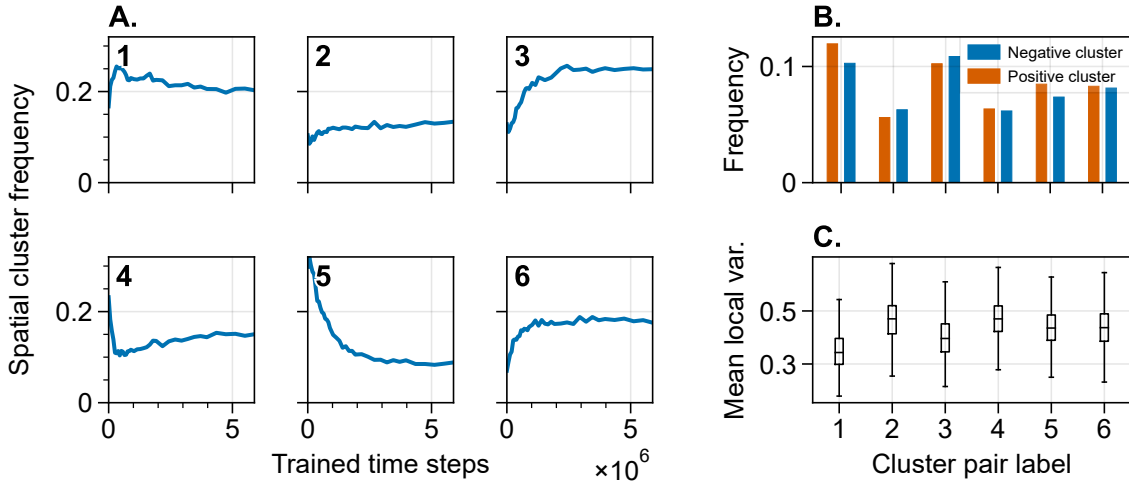


Figure 8: **A.** Spatial heatmap cluster labeling frequency over training. **B.** Comparison of frequencies of positive and negative cluster occurrences (where positive and negative are arbitrarily labeled as in Fig 7) **C.** Mean local variance measure for spatial heatmaps with a given cluster label. Boxplots are centered at the median, with the body going from the first quartile (Q1) to the third quartile (Q3). Whiskers are drawn at 1.5 inter-quartile ranges below and above Q1 and Q3 respectively.

common features used by agents at different skill levels and in different strategies. Individual nodes may be spatially noisy, but by combining inputs from a layer, these key features may be effectively transmitted through the network.

In Fig 9 we show a few spatial heatmaps alongside the clusters they are classified into (visualized by their centers). These demonstrate how cluster centers can contextualize what heatmaps that would otherwise be as noisy activations. The cluster visually clarifies the most notable features of a heatmap image, suggesting what information a node may be involved in providing to downstream computations in the network. This clustering approach enhances our understanding of spatial encodings by artificial agents, highlighting how their strategies evolve from using place-field-like behavior and tracking goal location, to using the corridor entrance as a key navigation feature. It also provides context to interpret the activations of nodes that might otherwise be dismissed as being noisy and not providing useful information. This kind of unstructured clustering strategy might have broader applicability to interpreting neuron recordings in biological studies, where data is often noisy. Later in Sec 3.4, we give another example of the effectiveness of analyzing populations of nodes in uncovering representations.

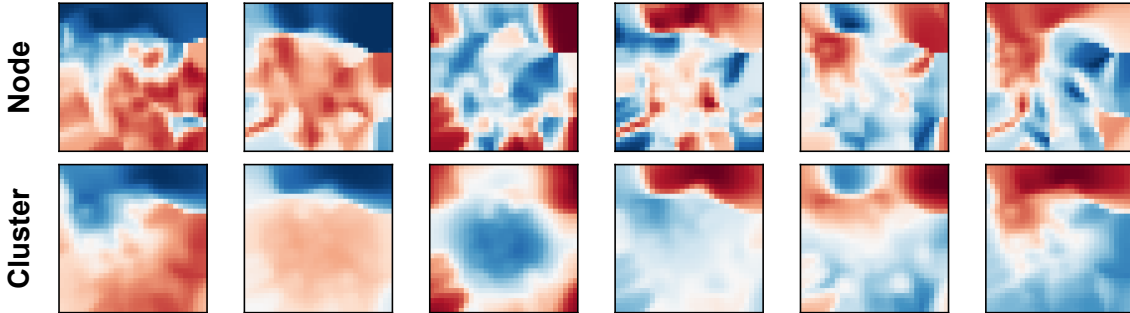


Figure 9: Examples of some spatial heatmaps with the corresponding cluster centers that they were assigned to. Each column corresponds to one node, with the node’s activity heatmap shown on the top, and the cluster center on the bottom. Nodes were selected from different agents.

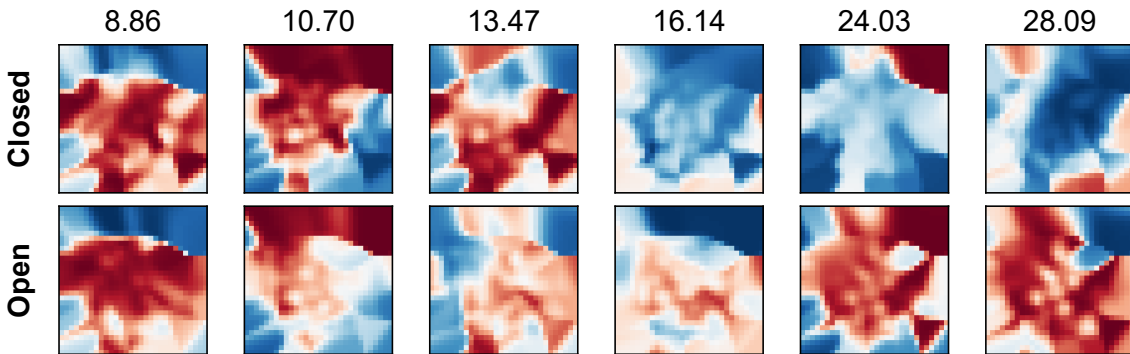


Figure 10: Examples of landmark sensitivity scores for a few nodes drawn from one  $p = 0.5$  agent late in training. Each column of 2 heatmaps are the spatial activity heatmaps for a single node from 50 closed shortcut episodes (top) and 50 open shortcut episodes (bottom). The number above the heatmap is the landmark sensitivity score for the node, which is calculated as the absolute difference of the two heatmaps.

### 3.3. Landmark Sensitivity Representation

The next representation we consider is landmark sensitivity, specifically measuring how responsive a node is to changes in an available visual landmark. Recall that the shortcut wall is colored purple unlike other white walls in the environment, and it acts as a salient cue when closed off. We hypothesized that having nodes with a robust representation of this landmark should correlate to an agent’s ability to recognize and utilize the open or closed state of the shortcut, and hence correlate with increased performance. This concept is inspired from humans, where the use of distal and proximal cues is important in navigation skills [3, 21].

To quantify a node’s sensitivity to the purple wall landmark, we compare its spatial activity heatmap from 50 closed shortcut episodes with the heatmap generated from 50 open episodes. A large difference between these two indicates high landmark sensitivity. This measure could alternatively be assessed by comparing average node activations between open and closed episodes, but spatial heatmaps offer a clear visual distinction in node responses under open and closed shortcut states, as seen in examples presented in Fig 10. We define a landmark score above 21 as indicative of clearly distinct heatmaps, such as the two right-most nodes shown in the examples.

Two key observations arise from this representation score. First, as shown in the subplots of Fig 11A and in the combined plot Fig 11B, there is an initial decrease in landmark sensitivity during the early stages in training, particularly for agents trained with  $p > 0.1$ . This period coincides with the same early period of training where spatial representations develop (as seen from the mean local variance in Sec 3.2.1). The dip suggests that early representation formation is dominated by learning basic navigation skills, rather than the development of distinct strategies for open and closed trials.

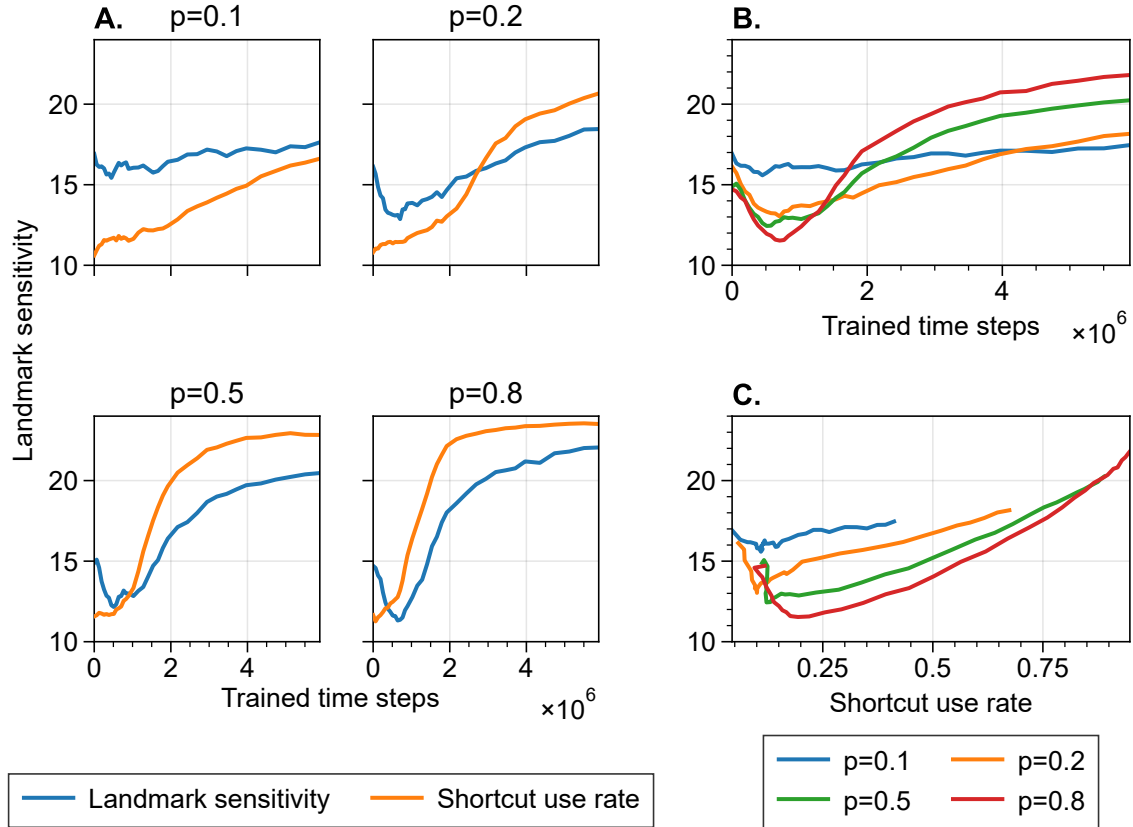


Figure 11: **A.** Comparison of shortcut use rate through training with cue sensitivity scores for individual  $p$  value agents. **B,** and **C** both show combined results on the same axis for multiple  $p$  values for comparison. **B.** Cue sensitivity across training time. **C.** Visualization of how cue sensitivity changes along with shortcut use rate.

The higher the  $p$ , the greater the dip in landmark sensitivity, parallel with less exposure to the landmark. On the other hand, the higher the  $p$ , the more landmark sensitivity is developed by the end of training.

Our second observation focuses on the correlation between shortcut use rates and landmark sensitivity scores, shown in Fig 11C. Towards the end of training, agents tend to converge toward optimal performance (100% shortcut use rate) and consistently develop average landmark sensitivity scores of around 23 (the plotted lines converging at the top right of the plot in Fig 11C) regardless of  $p$  value. With even more training, we expect agents from the lower  $p$  values of 0.1 and 0.2 might also develop towards this optimum. This convergence indicates that the development of landmark sensitivity is tightly coupled with shortcut taking strategies in our environment.

To conclude, we first observed a dip in landmark representation strength early in training, but increased exposure to the landmark (lower  $p$ ) mitigated the severity of this dip. We also noted that the landmark sensitivity is tightly coupled with shortcut use frequency, and higher  $p$  agents that learn to use the shortcut more effectively surpass lower  $p$  agents in landmark sensitivity scores after training. These insights suggest that while exposure to landmarks aids in developing representations, effectively integrating them into navigation strategies is more influential to building robust representations. These findings will later be contextualized with predictions for human navigators, where we propose that the dynamics of developing landmark knowledge in humans could mirror these dynamics observed in artificial agents.

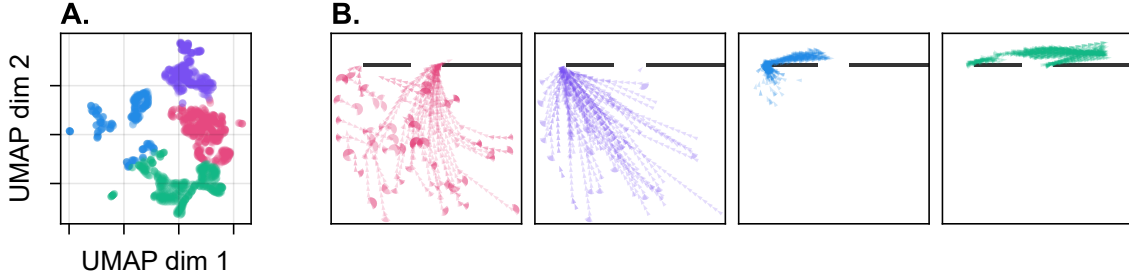


Figure 12: Example of k-means clustering data points from a  $p = 0.1$  agent late in training. **A.** Activations from the recurrent network layer reduced to 2 dimensions via UMAP and clustered according to k-means with  $k = 4$ . **B.** Each subplot shows where the agent was at time points corresponding to the clustered activation points.

### 3.4. Population level representations and agent “planning”

In this section, we expand our focus from individual node representations to those spanning an entire network layer. We use the same recurrent layer activations as before but analyze the combined activations of all nodes in the layer. Our preliminary exploration involved applying the nonlinear dimensionality reduction technique UMAP [13], reducing the set of  $T$  64-dimensional vectors (where  $T$  is the total number of time steps of data collected in all 100 episodes, and 64 is the number of nodes the layer) to  $T$  2-dimensional vectors that can be visualized. An example is given in Fig 12A.

To explore the structure of these population-level activations, we initially applied k-means clustering to the complete set of  $T$  2-dimensional activations. We then mapped out the positions of the agent corresponding to each clustered point. Fig 12 gives a visual demonstration of the process. This k-means clustering revealed that in well-trained agents, clusters frequently emerged that corresponded distinctly to different segments of the agent’s trajectory. The clearest separation of clusters in UMAP space distinguished times when the agent was above the corridor from points below, with clusters rarely containing both types of points. Additionally, clusters often formed such that points from trajectories where the agent took the long path and trajectories where the agent took the shortcut were placed in separate clusters (see example Fig 12).

These patterns formed the basis of a population-level representation which we explore further in the following discussion. This approach enables a broader understanding of how collective activations of neural network nodes correlates with an agent’s navigational decisions and strategic “planning” during navigation tasks.

#### 3.4.1. Quantifying trajectory set separation scores

We introduce a population-level representation score, attempting to quantify the idea of network activity separating in activation space based on the parts of a trajectory an agent was on. We first categorize data points from an agent into four sets as shown in Fig 13, noting that these sets are predefined and no longer apply k-means. Positions of the agent for each set are displayed in Fig 13B. From left to right, the first two sets contain points where the agent was below the corridor, and we call them “pre-entrance” (colored orange) if the agent took the longer corridor entrance path on that episode, or “pre-shortcut” (colored green) if the agent took the shortcut. The next two sets contain points where the agent was in the corridor, and similarly are termed “post-entrance” and “post-shortcut”, depending on which path the agent took on that episode. The set definitions are independent of whether the shortcut was actually open on a given episode. These sets aim to capture the “intent” or “plan” of an agent, rather than being based only on its spatial position. Positions in the “pre-entrance” and “pre-shortcut” sets, for example, highly overlap, but their activations in UMAP space can be well separated.

To measure the separation of these sets in activation space, we employ the Wasserstein distance, a metric that calculates the minimum sum of Euclidean distances between paired points in two sets. Let  $\{u_i\}$  be the points belonging to a set  $U$ , and likewise for  $\{v_j\}$  and  $V$ , where  $u_i$  and  $v_j$  are 64-dimensional activation vectors. The Wasserstein distance between  $U$  and  $V$  is defined as the sum

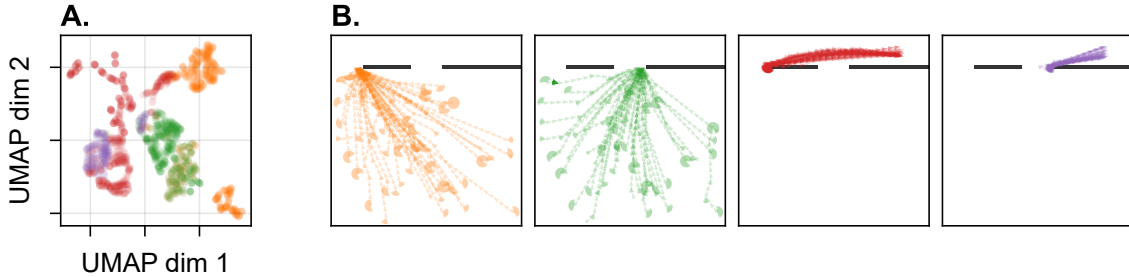


Figure 13: An example of population activity and position data from a  $p = 0.8$  agent late in training according to predefined trajectory sets. **A.** Activations collected over 50 open and 50 closed episodes of an agent performing its policy, reduced to 2 dimensions via UMAP for visualization. (Note that although hard to see, there is a region of overlap between green and orange points slightly towards the bottom-right of the plot.) **B.** Each subplot shows where the agent was at time points belonging to predefined sets. From left to right: pre-entrance, pre-shortcut, post-entrance, post-shortcut.

of distances between pairs  $(u_i, v_j)$  such that the distance  $\tilde{W} = \sum_{i,j} |u_i - v_j|$  is minimized. Each point is paired at most once, and all points from the smaller set are included in the calculation (some from the larger set may be left out). We normalize the Wasserstein distance by  $W = \tilde{W}/(N \cdot D)$  where  $N$  is the number of pairings, and  $D = \max |x_i - y_i|$  is the maximum Euclidean distance for any two points in the entire activation space.

We find that the most interesting set pair is the pre-entrance and pre-shortcut sets (the orange and green points in Fig 13) and is the *set separation score* that will be the main focus of our analysis. The separation score of this pair increases the most across training and has the best correlation with shortcut usage. In the example shown in Fig 13A, there are some distinct regions that only contain orange points in the top-right and bottom-right of the plot. There is also a region of overlap between the two clusters of interest slightly towards the bottom-right of the image. Notably, these sets separate quite well despite containing many points with similar positions.

Fig 14A tracks the development of this set separation score across training. There is a clear positive association between the set score and shortcut usage, as seen in Fig 14B, and unlike landmark sensitivity, this representation measure increases in a monotonic fashion. The separation of pre-shortcut and pre-entrance sets indicate that the population activity contains information about the intended route of the agent, and not merely the agent’s current position. Furthermore, the correlation of higher separation scores with improved performance indicates that this population-level representation which separates trajectories or strategies is useful in advanced navigation. We will inspect this idea more carefully in the next section.

### 3.4.2. Prescribed trajectories

We interpreted the pre-shortcut and pre-entrance separation score increasing as an indication of a neural network’s growing effectiveness in encoding trajectory or planning information. However, an alternate interpretation might suggest that this increase is not purely due to enhanced encoding abilities, but rather due to changes in policy during training that lead to modified visual inputs. For instance, an agent early in training that only takes shortcuts sometimes will end up with open shortcut episodes in both pre-entrance and pre-shortcut sets. On the other hand, an optimized, well-trained agent might have only open episodes in the pre-shortcut set and closed episodes in the pre-entrance set. The well-trained agent then would have more differing visual stimuli between the two sets, due to the landmark only occurring when the shortcut is closed. One might conclude that an increase in set separation after training is observed due to policy optimization that causes visual stimuli received in the two sets to differ.

Countering this interpretation, we observe that the set separation score continues to rise for  $p = 0.8$  agents even after performance has optimized and plateaued (at around  $2e6$  timesteps,  $p = 0.8$  agents use shortcuts about 90% of the time, from Fig 3C). This suggests that the population representation continues to strengthen despite stable visual stimuli. This is further evidenced in Fig

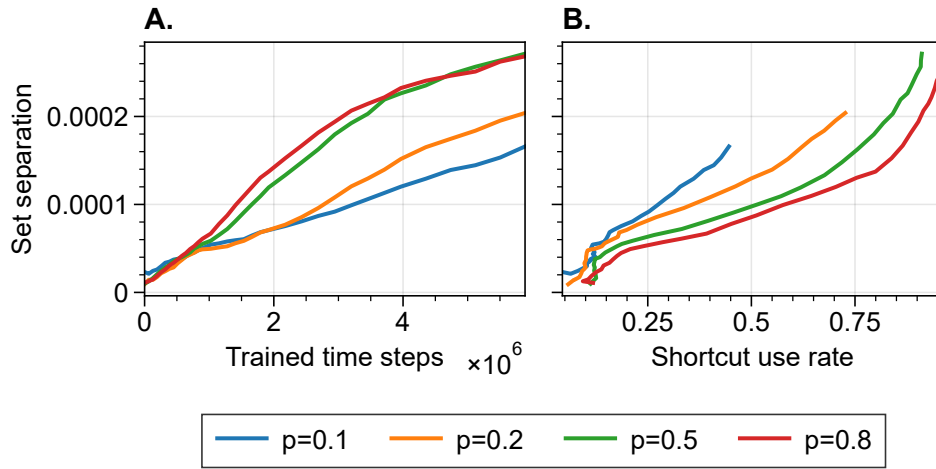


Figure 14: Wasserstein distances between pre-entrance and pre-shortcut network activation clusters. **A.** Mean Wasserstein distances across training. **B.** Visualization of how Wasserstein distance changes with respect to performance

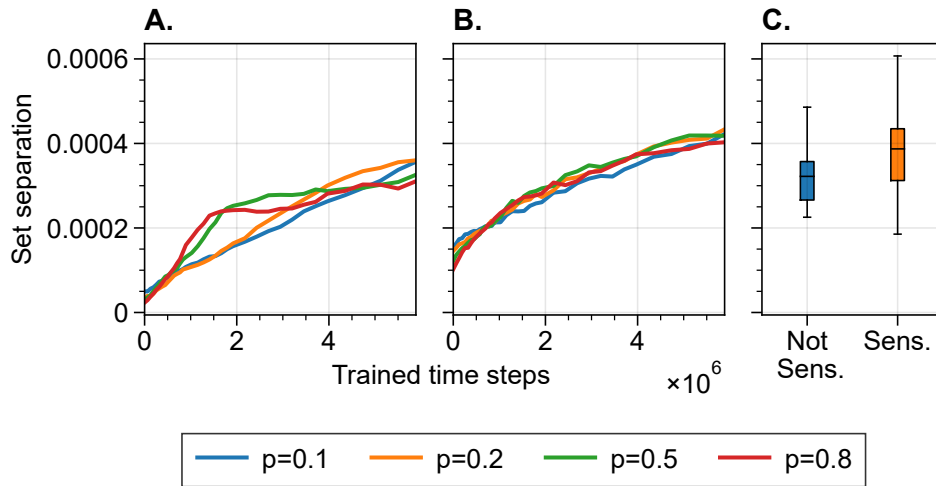


Figure 15: Wasserstein distances between activations from pre-entrance and pre-shortcut clusters. **A.** Mean Wasserstein distances only considering episodes where the shortcut was open. **B.** Mean Wasserstein distances using prescribed trajectories, open shortcut only. **C.** Boxplots showing Wasserstein set separation scores (policy trajectories, open episodes only) late in training while only considering cue sensitive nodes or non-cue sensitive nodes in sets.

15A, where we analyze separation scores exclusively using data from open shortcut episodes. The positive correlation between score and skill is still preserved, lending further evidence that agents are learning to encode trajectory information, and not merely reacting to differential visual stimuli.

To conclusively demonstrate that increased set separation is not only a reflection of changes to behavior, we employ a novel data collection strategy of prescribed trajectories. In this method, we copy the action history of one agent that had approximately 60% shortcut use rate, and then collect activations for all agents under those same actions. This allows us to observe how agents respond to a fixed set of behaviors and visual stimuli. Fig 15B illustrates that, even with controlled actions, agents progressively learn to distinguish between paths leading to the entrance versus the shortcut.

Interestingly, in both alternate measures of set separation shown in Fig 15A and 15B, the difference between different  $p$  agents is diminished or eliminated. This suggests that a more optimized policy does contribute to increased set separation score, along with better representation encoding. The key takeaway from this section is that agents learn representations at the population level that indicate an understanding of what trajectory they are headed towards, rather than just their current location. Although closely associated with shortcut usage, these representations also evolve independently of performance, continuing to mature even when policies are nearly optimal. Future research could explore the underlying mechanisms driving this continued representation development, potentially looking into what drives network gradients once earned reward signals have stabilized.

### 3.4.3. The role of landmark sensitive nodes in trajectory representations

In Sec 3.3, we identified nodes with a landmark representation score greater than 21 as particularly sensitive to the shortcut wall landmark. Fig 15C demonstrates that these landmark-sensitive nodes contribute more significantly to the separation of pre-shortcut and pre-entrance activations compared to non-sensitive nodes. This analysis only includes open shortcut episodes to minimize the impact of varying visual stimuli on the result.

This finding suggests that even in the absence of the landmark, landmark-sensitive nodes play a crucial role in shaping population-level representations. This could indicate their general importance in advanced navigation or trajectory planning. Alternatively, the landmark sensitivity measure might effectively identify nodes that consistently provide valuable navigational information to the rest of the network. It is not uncommon to observe some activations in a neural network layer to become less informative over RL training [11, 22], and representation scores may be a way to filter out “useful” nodes. These observations might warrant further study, potentially by examining more quantifiable representations to see if nodes scoring highly on those metrics also play pivotal roles in population codes.

To summarize this whole section, the detailed analysis of trajectory representations implies that agent networks are learning to encode information about “intended” trajectories. Additionally, the correlation between this score with performance is due to more than just differences of visual stimuli between sets. Even though many nodes have a strong spatial component, it is important for us to look at the population activity to derive predictive signals for the agent’s behavior. We have shown examples of population analysis and k-means being useful for discovering ways to interpret noisy activity patterns. We have also shown that population activity as a whole can encode information that is useful in an agent’s policy. This perspective of looking beyond individual nodes to sets could be useful beyond artificial agents, and may have value in understanding collections of spiking neural data, especially where the behavior of individual neurons is noisy and challenging to interpret.

### 3.5. Comparisons with human navigators

In this final section, we extrapolate findings from our analysis of artificial agents to human navigators. Our research was inspired by a study examining how the environment individuals live in affect their navigation skills and strategies [1]. Barhorst-Cates et al. assessed individuals from Salt Lake City and Padua on a number of different tasks, including the Dual Solutions Paradigm (DSP), designed to evaluate shortcut usage. Individuals from Padua were found to have a greater ability to use proximal cues during navigation than those from Salt Lake City as well as use shortcuts more often in the DSP.

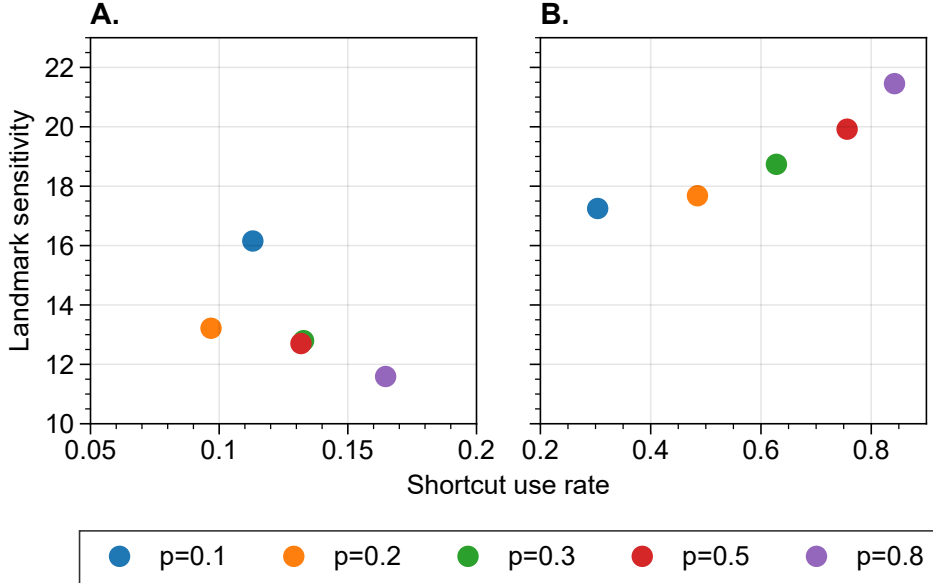


Figure 16: Comparison of landmark sensitivity scores with shortcut use rate at **A.** early in training, near the point of lowest cue sensitivity; **B.** near the end of training

Drawing parallels, we compare our  $p = 0.1$  agents to individuals from Salt Lake City, where grid-like street layouts offer few shortcuts, reflected by the sparse shortcut opportunities in the  $p = 0.1$  environment. On the other hand, Padua’s irregular and organic street layouts are rich in shortcut opportunities and is likened to the  $p = 0.8$  variation. As shown earlier in Fig 3, the higher the  $p$  an agent is trained in, the faster its performance was optimized. Similarly, Barhorst-Cates et al. found individuals from Padua to have generally better navigation skills than those from Salt Lake City. With this comparison, we make two predictions for human navigators and the environments that they live in.

### 3.5.1. A small increase in shortcut experience induces a large learning benefit

Referring back to Fig 3C, we observed a large gap in learning efficiency between agents from  $p = 0.1$  and  $p = 0.8$  environments. One might assume  $p = 0.2$  agents would resemble those from  $p = 0.1$ , with closed shortcut episodes dominating their experience. Yet, their learning dynamics and representation development, particularly the initial dip in landmark sensitivity, are more qualitatively similar to  $p = 0.5$  or  $p = 0.8$  agents. Additionally,  $p = 0.3$  agents reach nearly the same asymptotic performance as agents in  $p = 0.8$ , far beyond those from  $p = 0.1$ . This suggests that even small adjustments in training conditions can significantly influence learning outcomes. This could also be interpreted as navigation skills taking a critical amount of experience to develop.

While the learning mechanisms between humans and RL agents differ, we propose a modification to the DSP to test this hypothesis. Typically, DSP participants are first instructed to walk around the perimeter of a maze multiple times while noting the objects that they come across. Afterwards, they are tasked with finding their way to these objects, and the frequency that they use shortcuts in the maze (cutting through the maze, as opposed to following the path they were initially guided on) is recorded.

During the initial phase of guided exploration, we suggest incorporating some number of example paths where participants are led through the center of the maze. Based on our findings, we hypothesize that these demonstrations should induce a nonlinear improvement in the amount of shortcuts used by participants as a function of the number  $N$  of shortcut demonstrations given. In other words, as  $N$  is increased, we predict that initially a substantial increase in shortcut taking will be observed. Eventually though, the marginal benefit of increasing  $N$  further should taper off, with the most significant gains in shortcut usage coming from the first few additional demonstrations.



### 3.5.2. Dependence of representation and navigation skill development on environment

Landmark knowledge is usually regarded as beneficial for navigation in humans [3, 21]. In our artificial agents, we showed that this was certainly the case, where optimal navigation policies and robust landmark sensitive representations developed concurrently (see Fig 11C), particularly in agents trained with higher  $p$  values. Similarly, individuals from Padua were found to have better allocentric navigation skills and more ability to use proximal cues in navigation than those from Salt Lake City [1]. However, the amount of experience an individual had was not a main focus in that study.

In our deep RL agents, we found that the amount of training modulated the relationship between shortcut use and landmark sensitivity for across different  $p$  values. This result is highlighted in Fig 16, which depicts the relationship early and late in training. Early on, lower  $p$  agents showed better representation scores, due to the previously discussed dip in score that is mitigated by exposure to the landmark. However, as training progresses, the ordering reverses with higher  $p$  agents achieving higher representation scores. To interpret this observation for human navigators, we equate the training time of an agent to the amount of navigation experience a human has. Evaluating the agent is similar to running a DSP trial with a human, and the representation scores that we measure in agents can be thought of as generalizable skills that an individual has picked up (comparing landmark sensitivity score in agents to landmark knowledge in humans).

Mapping our findings from artificial agents to humans then suggests that the landmark knowledge an individual from Padua or Salt Lake City has should depend on the amount of navigational experience they have. If we were to compare individuals of less experience from both groups, then those from Salt Lake City (like our  $p = 0.1$  agents) should have higher landmark knowledge than those from Padua (like our  $p = 0.8$  agents), and the relationship should reverse when comparing individuals with greater experience. To empirically test this hypothesis, one could conduct a longitudinal study tracking individuals over time to evaluate changes in their landmark knowledge. Alternatively, a factorial experiment could be designed where individuals from different environments are subdivided based on various navigational skills, such as performance on the DSP, and landmark knowledge is compared across subgroups.

## 4. Discussion

Our work is strongly motivated by research into individual differences in navigation skill in humans. The goal was to apply deep RL agents as a model for behavioral studies of human navigators while also taking inspiration from navigation research to develop RL training environments and representation analysis techniques. For human navigators, we provide insight into the differences found in navigation ability based on where an individual grew up. Our findings with artificial agents suggest that engaging with landmarks in sufficiently challenging environments enhances the development of landmark sensitive representations. This is similar to the findings of individuals from Padua and Salt Lake City, where the former group generally has better landmark knowledge in an environment that is harder to navigate [1]. Importantly, our analysis predicts that differences between these groups may diminish or reverse when focusing on less experienced individuals. Separately, we also predict that introducing shortcut demonstrations into a DSP experiment might lead to non-linear improvements in shortcut use frequency based on the number of demonstrations given.

We make an important note that deep RL is an imperfect model to capture the complex learning dynamics of human or animal brains. While our insights and predictions can at best roughly translate from neural network representations to human navigational skills, they are intended to inspire testable hypotheses at a qualitative level. RL also has a history of being applied to interpret brain signals, like explaining dopaminergic neuron firing rates as a temporal difference signal [5]. In our work, we measure landmark sensitive nodes in the neural network by comparing activations (which can be thought of as similar to neuron firing rates) when a landmark is present to when it is not. This technique might also be applicable in brain recordings, for example by randomly removing an object in the DSP and looking for differential activity responses to mark cue sensitive neurons.

Another important discussion point is of best practices to analyze representations in artificial agents. Our primary approach involved recording activations while the agent performed its usual

policy on the task that it is trained in. This comes with the caveat that the policy that generates the trajectories itself influences the recorded activations by affecting inputs to the network, and could lead to misattributing behavioral changes to shifts in representation learning. As demonstrated in Sec 3.4.2, with artificial agents we have the option of feeding fixed, repeatable stimuli to the agent and seeing how the network responses change through training. However, we have noticed that controlling stimuli can diminish the strength of representations, and could lead to some encodings being missed entirely. In artificial agents, since representations are optimized as part of an agent’s policy, they should be considered valid within that context. Place cells, which serve as a main motivation, have also been found to be dependent on environment and task context [7, 14]. Thus, while using prescribed trajectories is a valuable technique to weigh the influence of policy changes in representation strength, representations should also be analyzed with the policies they are developed.

In our representation analysis, we began with inspiration from place cells [18], mapping out locations that individual nodes were sensitive to. One technique we highlight that runs counter to this paradigm is to analyze populations of cells as a way to understand neural encodings, rather than limiting exploration to just individual nodes. We apply k-means as one way to perform analysis on a group of nodes. In Sec 3.2.2, k-means revealed common spatial features that developed in navigation learning. When matching a heatmap to its nearest cluster, it often becomes much clearer what feature that node might help encode, and these features could be hard to glean from the individual node level. In Sec 3.4, applying k-means directly to UMAP-reduced node activations revealed the existence of a trajectory-based (or “planning-based”) representation, as opposed to position-based ones we had first searched for. The key takeaway is that looking at the population of activities or neural firing rates may be a useful exploratory tool to better understand what a network or brain is encoding. In the context of the whole population of activity, noisy individual node activations reveal themselves to be part of a larger picture of useful representations, and this perspective may be broadly valuable in analyzing neural recordings.

#### **Acknowledgements.**

We thank Dr. Sarah Creem-Regehr, Dr. Elliot Smith, Dr. Frederick Adler, and Dr. Akil Narayan for helpful discussions of this work. The support and resources from the Center for High Performance Computing at the University of Utah are also gratefully acknowledged.

#### **References**

- [1] Erica M Barhorst-Cates, Chiara Meneghetti, Yu Zhao, Francesca Pazzaglia, and Sarah H Creem-Regehr. Effects of home environment structure on navigation preference and performance: A comparison in veneto, italy and utah, usa. *Journal of Environmental Psychology*, 74:101580, 2021.
- [2] Marc Bellemare, Will Dabney, Robert Dadashi, Adrien Ali Taiga, Pablo Samuel Castro, Nicolas Le Roux, Dale Schuurmans, Tor Lattimore, and Clare Lyle. A geometric perspective on optimal representations for reinforcement learning. *Advances in neural information processing systems*, 32, 2019.
- [3] Chien-Hsiung Chen, Wen-Chih Chang, and Wen-Te Chang. Gender differences in relation to wayfinding strategies, navigational support design, and wayfinding task difficulty. *Journal of environmental psychology*, 29(2):220–226, 2009.
- [4] Kyunghyun Cho, Bart Van Merriënboer, Dzmitry Bahdanau, and Yoshua Bengio. On the properties of neural machine translation: Encoder-decoder approaches. *arXiv preprint arXiv:1409.1259*, 2014.
- [5] Jeffrey R Hollerman and Wolfram Schultz. Dopamine neurons report an error in the temporal prediction of reward during learning. *Nature neuroscience*, 1(4):304–309, 1998.
- [6] Michał Kempka, Marek Wydmuch, Grzegorz Runc, Jakub Toczek, and Wojciech Jaśkowski. Vizdoom: A doom-based ai research platform for visual reinforcement learning. In *2016 IEEE conference on computational intelligence and games (CIG)*, pages 1–8. IEEE, 2016.

- [7] Tsuneyuki Kobayashi, Hisao Nishijo, Masaji Fukuda, Jan Bures, and Taketoshi Ono. Task-dependent representations in rat hippocampal place neurons. *Journal of Neurophysiology*, 78(2):597–613, 1997.
- [8] Ilya Kostrikov. Pytorch implementations of reinforcement learning algorithms, 2018.
- [9] Andrew Liu and Alla Borisyuk. Investigating navigation strategies in the morris water maze through deep reinforcement learning. *Neural Networks*, 172:106050, 2024.
- [10] Clare Lyle, Mark Rowland, Georg Ostrovski, and Will Dabney. On the effect of auxiliary tasks on representation dynamics. In *International Conference on Artificial Intelligence and Statistics*, pages 1–9. PMLR, 2021.
- [11] Clare Lyle, Zeyu Zheng, Evgenii Nikishin, Bernardo Avila Pires, Razvan Pascanu, and Will Dabney. Understanding plasticity in neural networks. *arXiv preprint arXiv:2303.01486*, 2023.
- [12] Steven A Marchette, Arnold Bakker, and Amy L Shelton. Cognitive mappers to creatures of habit: differential engagement of place and response learning mechanisms predicts human navigational behavior. *Journal of neuroscience*, 31(43):15264–15268, 2011.
- [13] Leland McInnes, John Healy, and James Melville. Umap: Uniform manifold approximation and projection for dimension reduction. *arXiv preprint arXiv:1802.03426*, 2018.
- [14] Bruce L McNaughton, Francesco P Battaglia, Ole Jensen, Edvard I Moser, and May-Britt Moser. Path integration and the neural basis of the 'cognitive map'. *Nature Reviews Neuroscience*, 7(8):663–678, 2006.
- [15] Maayan Merhav and Thomas Wolbers. Aging and spatial cues influence the updating of navigational memories. *Scientific Reports*, 9(1):11469, 2019.
- [16] Piotr Mirowski, Razvan Pascanu, Fabio Viola, Hubert Soyer, Andrew J Ballard, Andrea Banino, Misha Denil, Ross Goroshin, Laurent Sifre, Koray Kavukcuoglu, et al. Learning to navigate in complex environments. *arXiv preprint arXiv:1611.03673*, 2016.
- [17] Volodymyr Mnih, Adria Puigdomenech Badia, Mehdi Mirza, Alex Graves, Timothy Lillicrap, Tim Harley, David Silver, and Koray Kavukcuoglu. Asynchronous methods for deep reinforcement learning. In *International conference on machine learning*, pages 1928–1937. PMLR, 2016.
- [18] May-Britt Moser, David C Rowland, and Edvard I Moser. Place cells, grid cells, and memory. *Cold Spring Harbor perspectives in biology*, 7(2):a021808, 2015.
- [19] Alina Nazareth, Xing Huang, Daniel Voyer, and Nora Newcombe. A meta-analysis of sex differences in human navigation skills. *Psychonomic bulletin & review*, 26:1503–1528, 2019.
- [20] John Schulman, Filip Wolski, Prafulla Dhariwal, Alec Radford, and Oleg Klimov. Proximal policy optimization algorithms. *arXiv preprint arXiv:1707.06347*, 2017.
- [21] Alexander W Siegel and Sheldon H White. The development of spatial representations of large-scale environments. *Advances in child development and behavior*, 10:9–55, 1975.
- [22] Ghada Sokar, Rishabh Agarwal, Pablo Samuel Castro, and Utku Evcı. The dormant neuron phenomenon in deep reinforcement learning. *arXiv preprint arXiv:2302.12902*, 2023.
- [23] Richard S Sutton and Andrew G Barto. *Reinforcement learning: An introduction*. MIT press, 2018.
- [24] Steven M Weisberg and Nora S Newcombe. Cognitive maps: Some people make them, some people struggle. *Current directions in psychological science*, 27(4):220–226, 2018.